Desalination and Water Treatment
www.deswater.com

doi: 10.5004/dwt.2020.26314

206 (2020) 250–262
December

Biosorption of Pb^{2+} and Cr^{3+} ions from aqueous solution by two brown marine macroalgae: an equilibrium and kinetic study

Heba S. Ali[a,*], Nabil Fathi El Sayed Kandil[a], Ibraheem B.M. Ibraheem[b]

[a]*Department of Ecology, Soils, Water and Environment Research Institute (SWERI), Agriculture Research Centre (ARC), P.O. Box: 175 El-Orman, Giza, Egypt, Tel. (+2) 01204431635; email: heba.abdelsalam@yahoo.com (H.S. Ali), Tel. (+2) 01006746350; email: nabilkandil53@gmail.com (N.F.E.S. Kandil)*
[b]*Botany and Microbiology Department, Faculty of Science, Beni-Suef University, Beni-Suef 62511, Egypt, Tel. (+2) 01011050808; email: ibraheemborie@gmail.com (I.B.M. Ibraheem)*

Received 15 October 2019; Accepted 29 June 2020

ABSTRACT

Heavy metals impose a potential threat against the aquatic environment. Lead (Pb^{2+}) and chromium (Cr^{3+}) are some of the most prevalent toxic cations in wastewaters. In this study, two species of brown seaweeds *Hydroclathrus clathratus* and *Cystoseira barbata* were examined to remove Pb^{2+} and Cr^{3+} ions from aqueous solution. The parameters that affect the biosorption equilibrium capacity and kinetics such as biomass dosage, pH, initial metal concentration, and reaction time were studied at room temperature. Results revealed that both metal ions uptake was increased progressively with increasing contact time, pH value, and sorbent dosage. The biosorption capacity was reduced with increasing concentrations of both metals. Maximum biosorption efficiency was achieved at 120 min, pH 5, and 10 g L^{-1}. The pseudo-second-order equation displayed good agreement with Pb^{2+} and Cr^{3+} biosorption data. The equilibrium data of Pb^{2+} and Cr^{3+} biosorption were successfully correlated to the Langmuir equation under the trial parameters. The Langmuir maximum uptakes of Pb^{2+} and Cr^{3+} biosorption are 4.97, 7.19 mg g^{-1} on *H. clathratus* and 4.61, 7.30 mg g^{-1} on *C. barbata*, respectively. The results obtained indicated that these seaweeds provide an eco-friendly alternative sorbent biomaterial for metal removal from contaminated water.

Keywords: Biosorption; Cr^{3+}; Pb^{2+}; Brown macroalgae; Isotherms; Kinetics

1. Introduction

A major ecological concern which necessitates adequate treatment and extensive study is the release of hazardous metal pollutants into water bodies [1,2]. Owing to their extremely poisonous impact on human health and the ecosystem, environmentalists are extremely interested in wastewater remediation technology [3,4]. In recent decades, industrial developments, such as mining, fertilizers, pesticide residues, paper, electronic, heating, and melting process, have directly led to the discharge of huge quantities of toxic metals into water resources, thus increasing water pollution and causing its scarcity [5,6].

Industrial and agricultural activities and poorly constructed drainage systems in Egypt are considered the main sources of pollution [7]. Level of metals in the water body and sediment of the River Nile in Egypt are greater than the permissible limits according to "the Egyptian General Authority for Standards and Quality Control" [8]. According to World Health Organization (WHO) guidelines, chromium and lead are heavy metals that are of great concern [9]. The maximum allowable limit for all metals in diverse systems has been determined by the WHO [10,11]. The widespread application of chromium in various industries such as electroplating, steel manufacturing, leather tanning, pigments, and corrosion protection industries, and

* Corresponding author.

glass manufacturers, have accounted for the release of Cr^{3+} in a trivalent oxidation state which has toxic and carcinogenic properties for living organisms [12,13]. Lead ions are considered toxins and a common pollutant found in the waste of the printing, mining, pigments, and battery industrial effluents [14,15]. Consequently, appropriate treatment of effluents containing Pb^{2+} and Cr^{3+} ions prior to being discharged into receiving water systems, is of great value as regards environmental quality and human health.

Marine macroalgae (seaweeds) are promising natural biomass resources that have high metal removal efficiency [16–19]. They have different bioactive phycochemicals such as polyphenols, polysaccharides, lipids, proteins, vitamins, and carotenoids which have several negative charge active groups, for example, carboxyl, phosphate, amine, and hydroxyl that create strong links between them and hazardous metals [20–22]. Therefore, brown seaweeds act as important normal exchangers for the removal of hazardous cations [23].

Diverse remediation technologies have been developed and used for the removal of hazardous pollutants like evaporation, reverse osmosis, evaporation, chemical precipitation, membrane filtration, reverse osmosis, electrochemical treatment, and ion exchange technologies [11,14]. Among these mechanisms, the biosorption process is considered one of the most eco-friendly, high capacity, and low-cost techniques applied to wastewater polluted with poisonous metals [24,25].

The present work objective is to examine the experimental parameters including solution pH, biomass dosage, initial metal concentration, and reaction time on the sorption capacity of Pb^{2+} and Cr^{3+} ions by *Hydroclathrus clathratus* and *Cystoseira barbata*. Two established kinetic models "pseudo-first-order and pseudo-second-order" and isotherm models "Langmuir and Freundlich" were applied to the biosorption study. Finally, the surface structure and mechanism of *H. clathratus* and *C. barbata* before and after Pb^{2+} and Cr^{3+} ions biosorption were also examined by means of "Fourier transform infrared spectroscopy (FTIR)" and "scanning electron microscopy (SEM)" with energy dispersive X-ray microanalysis (EDX). The findings indicated that there is insufficient researches on *H. clathratus* for the removal of Pb^{2+} and Cr^{3+} in the literature and furthermore, that the information available concerning biosorption with *C. barbata*, remains scarce.

2. Materials and methods

2.1. Preparation of biomass (brown marine macroalgae)

The brown marine macroalgae *H. clathratus* and *C. barbata* (Phaeophyta) used in the present study were collected from Al Quşayr city, the Red Sea, Egypt during the spring season. The marine algal samples were placed in isothermal plastic bags in a cooler tank on ice containing some local water then transferred to the laboratory. The collected algal species were carefully washed with tap water to clean them of unwanted materials such as debris and sand particles then rinsed well with distilled water. Subsequently, they were oven-dried at 60°C for 24 h. The dried biomass samples were screened through a sieve after crushing by a laboratory blender in order to select particles that were between 0.5 and 1 mm. The algal samples were kept for further use.

2.2. Preparation of Pb^{2+} and Cr^{3+} ions solution

Stock solutions (1,000 mg L^{-1}) of Pb^{2+} and Cr^{3+} ions were employed in this study as different concentrations of working solutions were made in the range of 5–50 mg L^{-1} from the stock solution. The standard chemical reagent solutions (Sigma-Aldrich) were of analytical grade and were supplied by Ireland. Different pH levels of the working solution were adjusted by adding drops of HCl or NaOH (0.1–1 M) solutions using a pH instrument, after the addition of the biomass. The equilibrium concentrations of Pb^{2+} and Cr^{3+} ions in solution were determined using an "inductively coupled plasma-optical emission spectrometer" (ICP-plasma JY.ULTIMA 2).

2.3. Biosorbent characterization

Raw and metal loaded biosorbent samples were filtered, then dried after being mixed with 20 mg L^{-1} of Pb^{2+} and Cr^{3+} ions at pH 5. The samples were examined using (JASCO-6100 model, Japan-FTIR spectrometer) at a 400–4,000 cm^{-1} wavelength range. The FTIR spectroscopic method was performed to define the active functional sites on the biosorbent surface. The properties of unloaded and Pb^{2+} and Cr^{3+} loaded biomass surface were studied using SEM with EDX using (JEOL, JSM-52500 LV SEM, Japan). SEM was used to visualize and characterize the surface microstructure of biomass cell surface, whilst EDX analysis was employed to understand the mechanism of the biosorption process and also to define the elements present on the biosorbent wall [26].

2.4. Pb^{2+} and Cr^{3+} biosorption studies

Lead (Pb^{2+}) and chromium (Cr^{3+}) sorption experiments were completed by mixing biosorbent material (1 g) with 100 mL of Pb^{2+} and Cr^{3+} synthetic solutions (20 mg L^{-1}) in 250 mL beakers so as to determine the optimum pH value and desired contact times. The beakers were agitated at 200 rpm on a mechanical shaker for 2 h at 25°C. The biosorption solution was subsequently centrifuged for 5 mins at 5,000 rpm to separate the suspended solids of biomass material. The equilibrium concentrations of Pb^{2+} and Cr^{3+} in solution were determined using an "inductively coupled plasma-optical emission spectrometer" (ICP-plasma JY.ULTIMA 2).

To determine the optimum pH value and its effect on metal ions biosorption, the medium pH ranged between alkaline, neutral, and acidic (pH range of 2–8) and the remaining concentrations of Pb^{2+} and Cr^{3+} ions were measured after the sorption experiment using 2.5 g of the different biomasses at initial concentrations (20 mg L^{-1}) of Pb^{2+} and Cr^{3+} ions. To achieve suitable pH values, we controlled the pH by the addition of diluted HCL and NaOH solutions.

To detect the influence of contact time, the biosorption investigations were conducted at diverse time intervals of 0, 10, 20, 30, 40, 60, 120, 180, 240, and 300 min using 2.5 g of the

different biomass materials at an initial metal concentration of 20 mg L^{-1}.

The effect of different Pb^{2+} and Cr^{3+} concentrations were also investigated using 2.5 g of the different biomass materials at different concentrations of initial metal ions of 5, 15, 20, 30, 40, and 50 mg L^{-1} to study the biosorption isotherms.

The effect of biomass doses on the biosorption process was detected by measuring the remaining concentrations of Pb^{2+} and Cr^{3+} ions (at 20 mg L^{-1} as initial concentration) by using different biosorbent amounts (0.2, 0.4, 0.6, 0.8, 1, 1.2, and 1.4 g) in the experiment.

The mathematical equations for Pb^{2+} and Cr^{3+} removal efficiency (R %), sorption uptake at studied time t (q_t, mg g^{-1}) and equilibrium (q_e, mg g^{-1}) are given by:

$$\% R = \frac{\left(C_0 - C_{eq}\right)}{C_0} \times 100 \quad (1)$$

$$q_t = \frac{\left(C_0 - C_t\right)V}{m} \quad (2)$$

$$q_e = \frac{\left(C_0 - C_{eq}\right)V}{m} \quad (3)$$

where C_0 (mg L^{-1}) is the initial Pb^{2+} and Cr^{3+} metal concentration, C_t (mg L^{-1}) is concentrations at studied time t, C_{eq} (mg L^{-1}) is the metal concentrations at equilibrium, V (L) is the aqueous solution volume, and m (g) is the amount of biomass [18,27,28].

3. Results and discussion

3.1. Biomass characterization

3.1.1. Fourier transform infrared spectroscopy

Fig. 1 presents the FT-IR spectral analysis of the studied *H. clathratus* and *C. barbata* before and after Pb^{2+} and Cr^{3+} sorption. The most intense and broad peak observed at 3,779.8 cm^{-1} typically refers to O–H groups that may be one of the cell wall components of raw *H. clathratus* and *C. barbata* [29]. The sorption peak at 3,434.5 cm^{-1} may correspond to N–H stretching vibration active groups of proteins in *C. barbata* that appears to shift after Pb^{2+} sorption to 3,436.6 cm^{-1} and after Cr^{3+} sorption to 3,440.4 cm^{-1}. The peak 2,927.4 cm^{-1} can be assigned to symmetric C–H stretching vibrations of the aliphatic functional groups in *C. barbata* which may be shifted to 2,925.5 cm^{-1} after Cr^{3+} biosorption. The stretching vibration peak of the amide group at 2,277.5 cm^{-1} may shift to 2,061.5 cm^{-1} after Cr^{3+} biosorption by *H. clathratus*. Both observed peaks at 1,436 and 1,421.3 cm^{-1} that signify symmetric C=O shifted to 1,430.9 and 1,425.1 cm^{-1} after Pb^{2+} biosorption by *H. clathratus* and *C. barbata*, respectively. This shift can be described by the association of the carboxyl functional group with Pb^{2+} [30]. The peaks assigned to C–O stretching may be shifted from 1,027.9 and 1,039.44 cm^{-1} to 1,025.9 and 1,024 cm^{-1} by *H. clathratus* and to 1,025.9 and 1,035.6 by *C. barbata* after Pb^{2+} and Cr^{3+} sorption, respectively. Conversely, the small peak corresponding to the S=O groups was shifted from 875.5 to 873.6 cm^{-1} after Pb^{2+} and Cr^{3+} biosorption by *C. barbata*. Moreover, the band at 669.2 cm^{-1} which corresponds to C–C bonds also shifted to 659.5 and 665.3 cm^{-1} after biosorption of Pb^{2+} and Cr^{3+} by *C. barbata*, respectively. The peaks below 600 cm^{-1} are fingerprint region and could be assigned to the phosphate or sulfur groups [21,31]. The small peaks located at 553.5 and 584.3 cm^{-1} were shifted to 584.3 and 588.2 cm^{-1} after Pb^{2+} biosorption by *H. clathratus* and *C. barbata* and to 547 cm^{-1} after Cr^{3+} biosorption by *H. clathratus*, respectively. By contrast, loaded biomass shows bonds creation and destruction.

Fig. 1 demonstrates the appearance of different bands at 2,073.1; 1,386.6; 428.1; and 435.8 cm^{-1} while the disappearance of the absorption bands at 3,779.8; 2,277.5; 1,120.4; 869.7; 709.7; and 584.3 cm^{-1}, suggested that hydroxyl, amino, carboxyl, phosphate, and sulfonate groups could contribute to Pb^{2+} and Cr^{3+} biosorption by *H. clathratus* and *C. barbata*. The main sources of these stretching frequencies observed by several references are listed in Table 1. From the current results, many active sites on the biomass surface act as binding positions for Pb^{2+} and Cr^{3+} ion sorption.

3.1.2. SEM analysis coupled with EDX microanalysis

The possible superficial morphology and metal interactions of the studied biomass can be indicated using SEM micrographs with EDX of *H. clathratus* and *C. barbata* taken before and after Pb^{2+} and Cr^{3+} biosorption (Fig. 2). We observed that the surface morphology of raw *H. clathratus* indicates a porous structure but some vacancies for raw *C. barbata* with rough and heterogeneous structures.

The SEM micrograph of Pb^{2+} and Cr^{3+} loaded biomass surface revealed a completely different morphology. Furthermore, pores facilitate a good possibility of metal ions biosorption [32,33]. After the biosorption of Cr^{3+}, the surface pores structure of *H. clathratus* was enclosed, while it exhibited a spongy and honeycomb structure after Pb^{2+} sorption. The surface of *C. barbata* became soft and had a poorly porous morphology in conjunction with an irregular surface format after Cr^{3+} biosorption, whereas the micrograph of Pb^{2+} loaded *C. barbata* demonstrated a complicated mass of filaments in a mesh form structure. It is evident that the structures of *H. clathratus* and *C. barbata* varied after the biosorption process.

EDX of biomass material before and after Pb^{2+} and Cr^{3+} sorption is shown in Fig. 3. To decide whether ion exchange is one of the main mechanisms of Pb^{2+} and Cr^{3+} biosorption by *H. clathratus* and *C. barbata*, the chemical structure, and reductions of inorganic elements, such as Na^{+}, Ca^{+}, Mg^{2+}, and Fe^{2+} were measured by EDX in raw and metal loaded studied biomass samples. The main components of the *H. clathratus* cell wall are Ca (18.4%), O (53.47%), and C (18.39%) in addition to small quantities of Na (4.74%), S (3%), and Cl (2%). The main cell wall elements of *C. barbata* are Ca (33.85%), C (10.77%), and O (49.02%) and small quantities of Mg (1.39%), Cl (1.39%), Na (2.69%), and K (0.88%).

After the biosorption process, several cations that were originally present on the matrix of *H. clathratus* and *C. barbata* cell wall were substituted by Pb^{2+} and Cr^{3+} ions, which confirm that Pb^{2+} and Cr^{3+} biosorption on the biomass surface has taken place. Following Pb^{2+} biosorption,

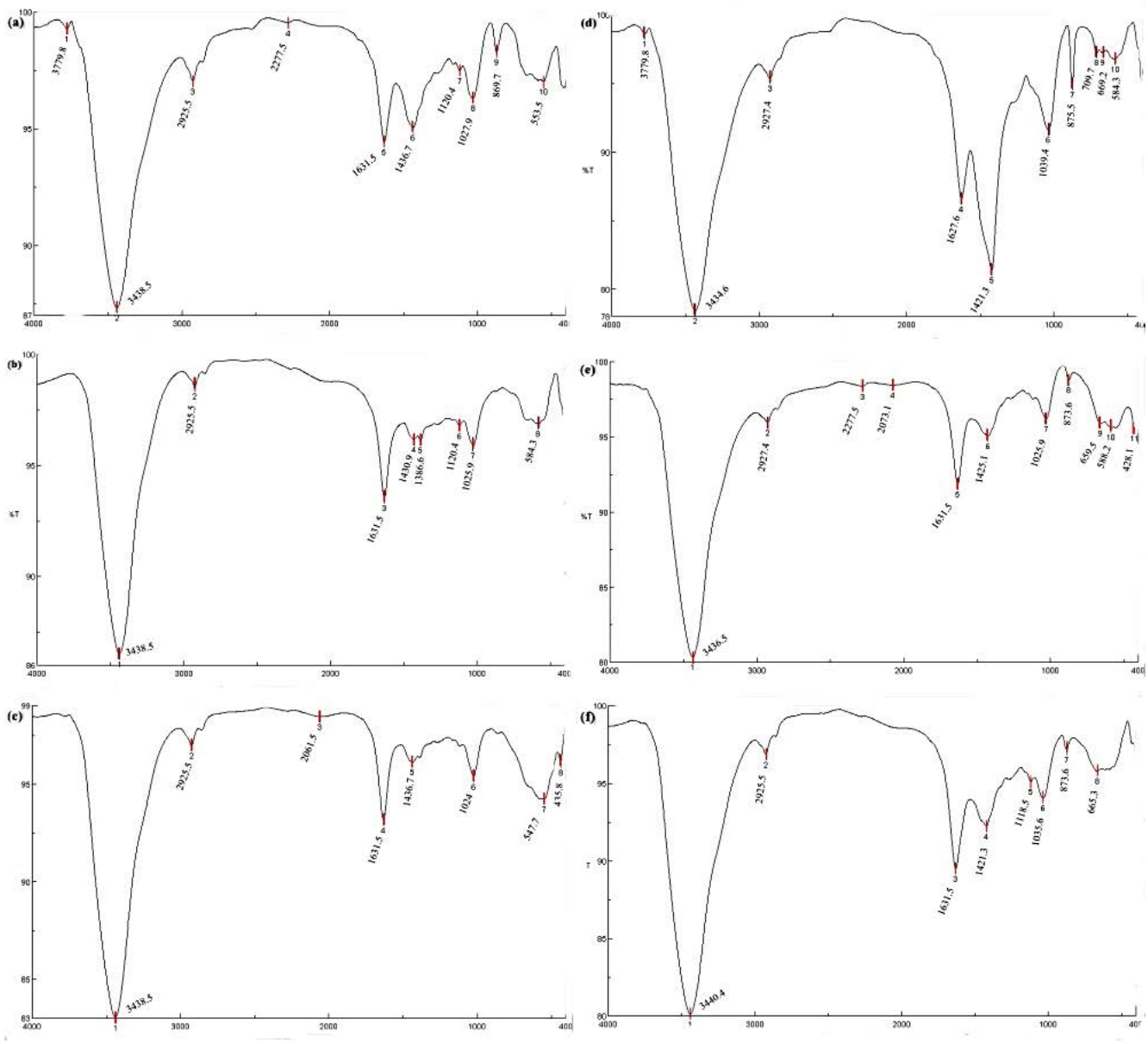

Fig. 1. FTIR pattern of *Hydroclathrus clathratus* (a) raw, (b) after Pb^{2+} biosorption, (c) after Cr^{3+} biosorption and *Cystoseira barbata* (d) raw, (e) after Pb^{2+} biosorption, and (f) after Cr^{3+} biosorption.

Table 1
Stretching frequencies observed in macroalgae FTIR spectra

Wave number (cm^{-1})	Assignment	Reference
3,440	N–H stretching vibration (amino or amide) functional sites of proteins	[25]
2,927	$–CH_2$ distention of aliphatic bonds, symmetric, and asymmetric stretching vibrations	[25]
2,277	$–NH^{2+}$, $–NH^{+}$, and –NH stretching vibrations functional groups	[24]
1,436	Stretching vibration of carboxyl groups –C=O (symmetric)	[21]
1,386	Asymmetric $–SO_3$ streching	[53]
1,120	(Ether) C–O	[53]
1,027	Alcohols and carboxylic acids C–O stretching	[24]
875	S=O stretch	[54]
669	C–C group present at the aromatic portion of the biomass structure	[25]

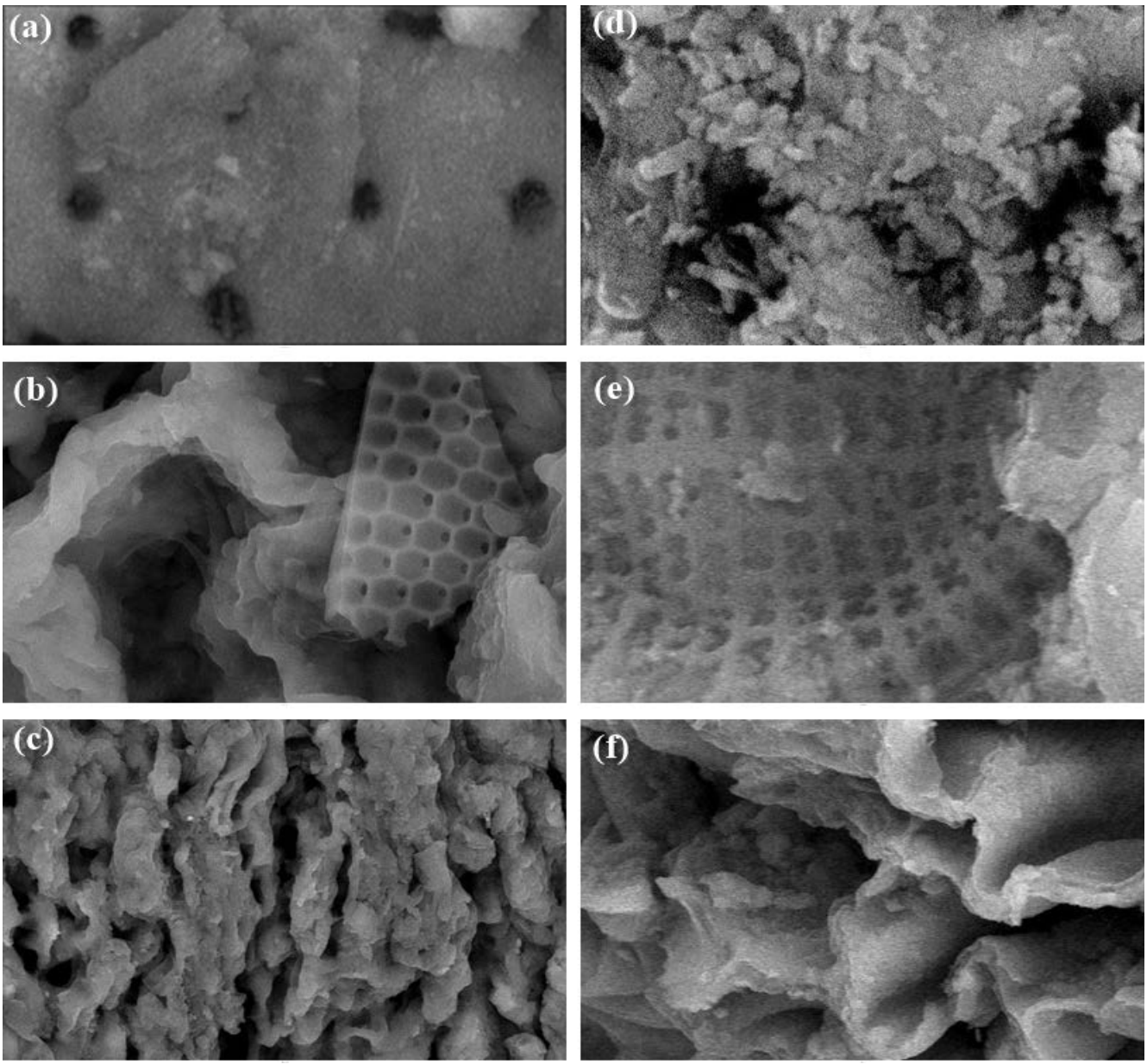

Fig. 2. SEM electron micrographs for *Hydroclathrus clathratus* (a) raw, (b) after Pb^{2+} biosorption, (c) after Cr^{3+} biosorption and *Cystoseira barbata* (d) raw, (e) after Pb^{2+} biosorption, and (f) after Cr^{3+} biosorption.

the amount of Ca in *H. clathratus* has decreased from 18.4% to 12.55% and from 33.85% to 12.09% in *C. barbata*. There is a minor decrease in Ca after Cr^{3+} biosorption by *H. clathratus* from 18.4% to 17.49% and a reduction in Ca after Cr^{3+} biosorption by *C. barbata* from 33.85% to 22.59% has been detected. The reduction in Ca suggests that ion exchange is conceivably one of the mechanisms responsible for the metal ion uptake by biomass. Lou et al. [27], observed the presence of Na, K, Mg, and Ca peaks in the raw brown algae *Laminaria japonica* from EDX analysis. Verma et al. [34], concluded that the major components of the cell wall of brown seaweed *Sargassum filipendula* are Na, Mg, K, and Ca and that some cations present on the cell wall were replaced by Pb^{2+} ions after the occurrence of the biosorption process. The cell wall functional groups of biomass are naturally occupied by K^+, Na^+, Ca^{2+}, and Mg^{2+} cations which persists in seawater at a high concentration [22]. The amount of metal ions bound to the raw biosorbent was similar to the light metal amount released by biomass [35].

3.2. Mechanism of metal biosorption by biomass

The biosorption of Pb^{2+} and Cr^{3+} ions occurred due to active function groups on the biomass cell wall. Thus, there are various functional and chemical active sites that can attract and secure metal ions where the biomass cell wall selects metal according to the surrounding area, such as the metal components and concentrations found

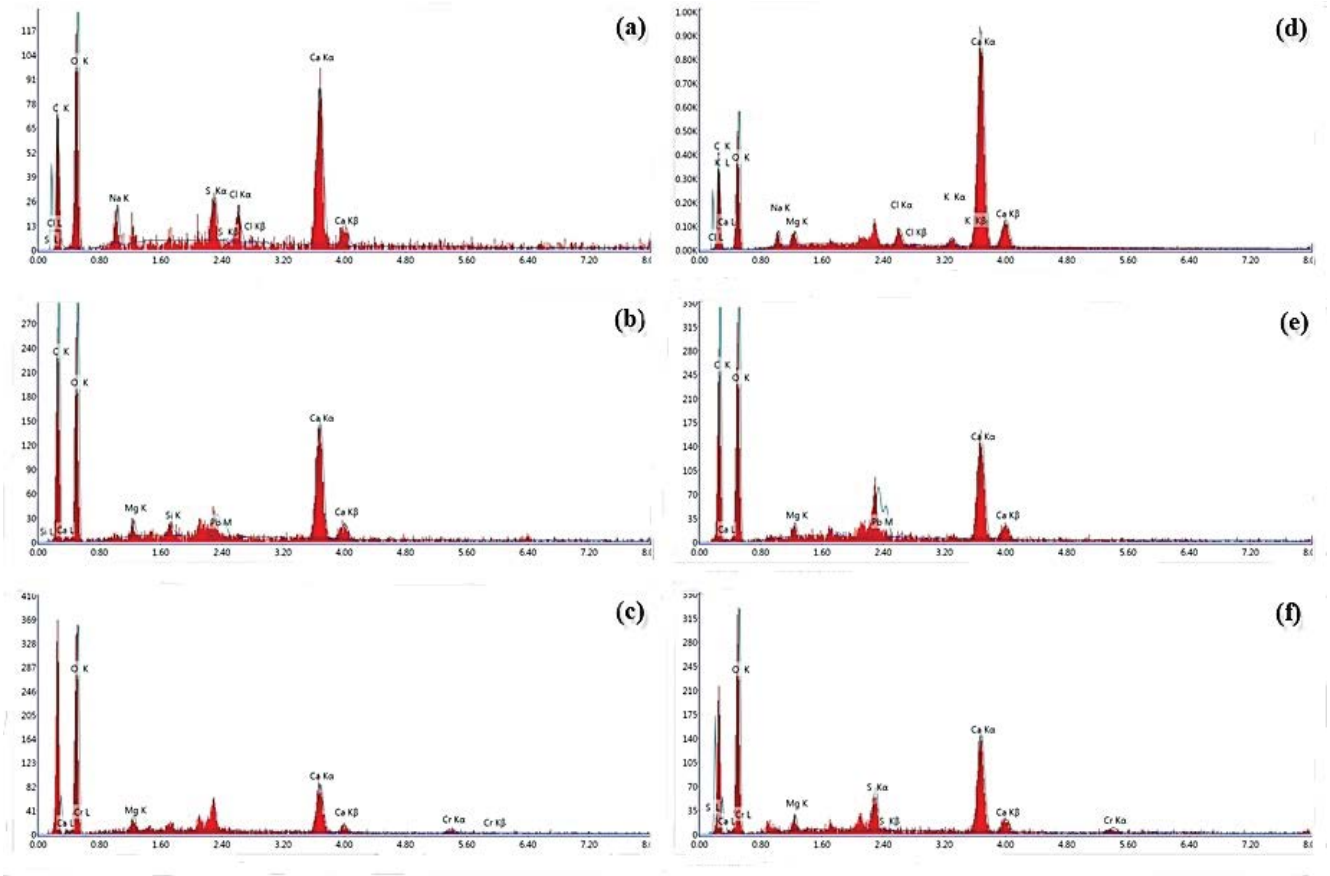

Fig. 3. EDX spectra of *Hydroclathrus clathratus* (a) raw, (b) after Pb^{2+} biosorption, (c) after Cr^{3+} biosorption and *Cystoseira barbata* (d) raw, (e) after Pb^{2+} biosorption, and (f) after Cr^{3+} biosorption.

in aqueous solution [22]. These adsorptive sites contain carboxyl, carbonyl, amide, hydroxyl, amine, and sulfonate groups as explained in the FTIR pattern. The significance of the given active groups for metal biosorption by biomass is governed by (1) the chemical state of the active sites, (2) the biomass reactive site numbers and availability of these sites, and (3) attraction between the sites and pollutant metals of interest [36]. The connection of Pb^{2+} and Cr^{3+} metal ions to the studied biomasses was achieved by bonds formation between metal ions and active sites in the bioactive components. The shifts occurred in the biosorption bands of the amine and hydroxyl groups in the FTIR analysis explained by the creation of the bonds between metal ions and sorbent materials (Table 1). The band shifts are as a result of the metal complex creation among the active functional sites and metal ions; those bands of active functional groups were shifted to higher or lower band numbers after the biosorption of metal ions [26,37].

3.3. Biosorption studies

3.3.1. pH effect on Pb^{2+} and Cr^{3+} biosorption

The pH value appears to be the most significant determining parameter affecting the biosorption process of metals. In this study, Fig. 4 shows the initial pH effect on the Pb^{2+} and Cr^{3+} biosorption efficiency by *H. clathratus* and *C. barbata*. As shown, the Pb^{2+} and Cr^{3+} removal efficiency (*R* %) progressively increases as the pH increases to pH 5 and then decreases at higher pH values. At pH 5, *H. clathratus and C. barbata* showed that the optimum value of Cr^{3+} biosorption efficiency was 93.18% and 82.22%, respectively. Similarity, the maximum Pb^{2+} biosorption efficiency by *H. clathratus* and *C. barbata* was 98.76% and 97.15%, respectively, at pH 5. The relationship between metal cations biosorption and the pH of the solution can be explained by the protonation or deprotonation phenomenon which takes place on the biosorbent surface [38]. The cations biosorption is inhibited at very low pH levels (acidic) as a result of the competition between the hydronium ions (H^+) and Pb^{2+} and Cr^{3+} ions for the functional sites. Therefore, the ligands of the cell wall are linked with positive hydronium ions [35,39,40]. However, with the additional increase in pH value, further ligands are exposed and the number of negatively charged deprotonated active sites increases, preferring the uptake of the cations [25]. In contrast, the biosorption efficiency decreases at pH > 6 because the solid phase hydroxide complexes of Pb^{2+} ($Pb(OH)_2$) and Cr^{3+} ($Cr(OH)_3$) were formed in the medium leading to precipitation [13,25,35]. According to our results, all the experiments were performed at the pH level for Pb^{2+} and Cr^{3+} solutions (~5.5) as an optimal level.

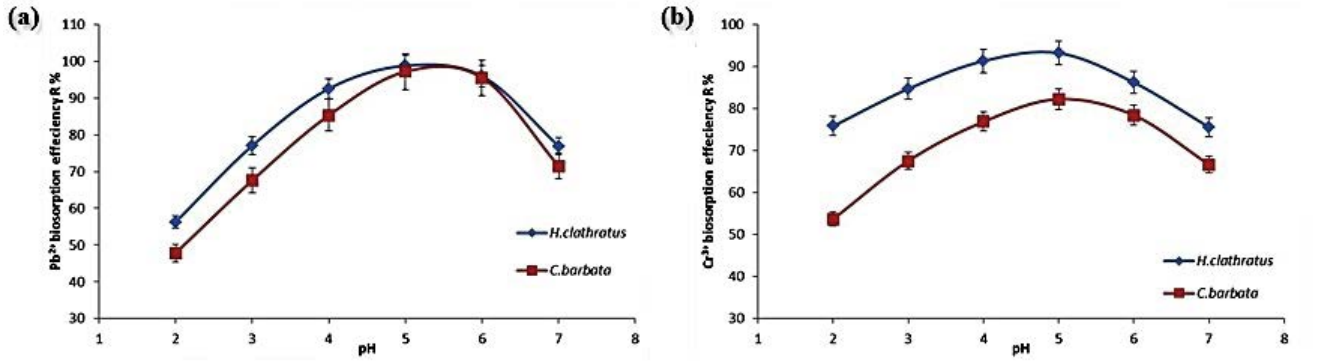

Fig. 4. pH effect on (a) Pb^{2+} and (b) Cr^{3+} biosorption efficiency *R* (%) of *Hydroclathrus clathratus* and *Cystoseira barbata* (*m*: 10 g L^{-1}; *V*: 100 mL; *t*: 120 min, and *T*: 25°C). The data are the mean of three replicate readings ± SD.

3.3.2. Effect of biosorbent amounts on Pb^{2+} and Cr^{3+} biosorption

The influence of the biosorbent amount on Pb^{2+} and Cr^{3+} sorption was investigated in the range of 2–16 g, as seen in Fig. 5. Our results exhibited that the efficiency of the biosorption process *R* (%) improves by increasing the biosorbent dosage of biomass up to 10 g. The sorption efficiency *R* (%) of Cr^{3+} increased from 82.59% to 93.55% by *H. clathratus*, and from 65.75% to 83.16% by *C. barbata*. Similarly, the biosorption efficiency *R* (%) of Pb^{2+} increased from 96.43% to 98.85% by *H. clathratus*, and from 95.14% to 97.27% by *C. barbata*. This is primarily due to the capability of the biosorption sites and superficial area of biomass, which accordingly increases the availability of more biosorption exchangeable sites onto the biomass [35]. However, the removal efficiency of Pb^{2+} and Cr^{3+} ions was practically the same and the biosorption increased till the biomass dose reached 10 g. It subsequently remained constant and did not increase further. Thus, it is apparent that a further increase in biomass dosage above 10 g does not increase biosorption efficiency.

This finding might be attributed to a reduction in the effective superficial area and biosorption sites of biomass for the metal ion uptake due to an aggregation of bisorbent at high concentrations of biosorbent material [18]. Therefore, 10 g was preferable as an ideal biosorbent dosage for effective biosorption.

3.3.3. Effect of reaction time on Pb^{2+} and Cr^{3+} biosorption

The biosorption efficiency *R* (%) of Pb^{2+} and Cr^{3+} ions by *H. clathratus* and *C. barbata* is illustrated in Fig. 6. At the early stages of the biosorption process, the removal efficiency was rapid; nearly 90% of the total Pb^{2+} and Cr^{3+} ions biosorption take place within the first 60 min then reach the maximum equilibrium stage after 120 min. After this faster step, the biosorption rate remained virtually constant and there was no further considerable change in the biosorption process up to 240 min. The metal uptake was faster during the initial stage due to the availability of large amounts of surface vacant groups. Thus the occupancy of the remaining unoccupied sites will be difficult owing to the repulsive forces between Pb^{2+} and Cr^{3+} ions on the solid biomass material and contaminated aqueous solution [35,41]. The observed rapid removal efficiency *R* (%) also has significant practical importance due to its benefits as an application method for real wastewater treatment plants.

3.3.4. Effect of initial Pb^{2+} and Cr^{3+} concentration

Initial Pb^{2+} and Cr^{3+} ions concentration effect were studied in the range of 5–50 mg L^{-1} at predetermined optimum conditions in Fig. 7. In this study, higher Pb^{2+} and Cr^{3+} concentration values would increase the specific biosorption capacity of metal ions but lower the biosorption efficiency percentage.

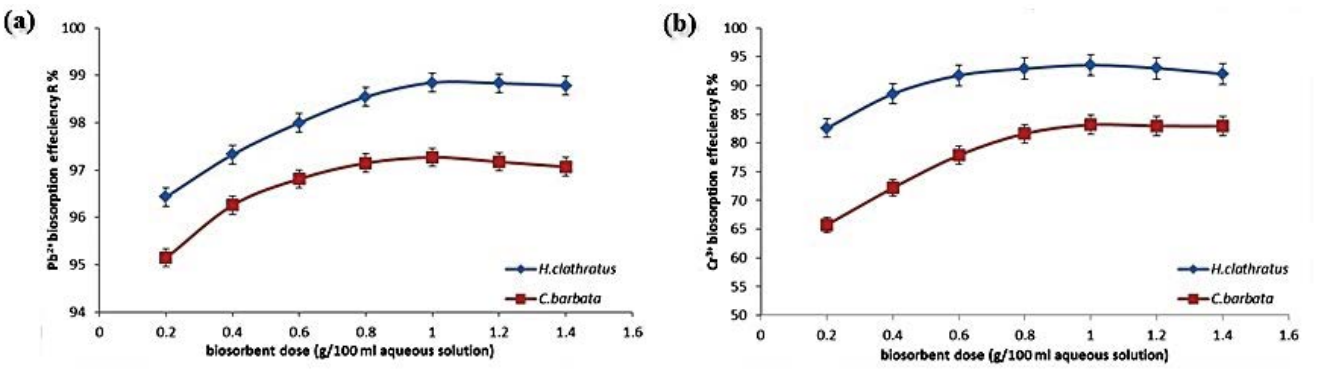

Fig. 5. Effect of biosorbent dose on (a) Pb^{2+} and (b) Cr^{3+} biosorption efficiency *R* (%) of *Hydroclathrus clathratus* and *Cystoseira barbata* (*T*: 25°C; *V*: 100 mL; *t*: 120 min, and pH: 5). The data are the mean of three replicate readings ± SD.

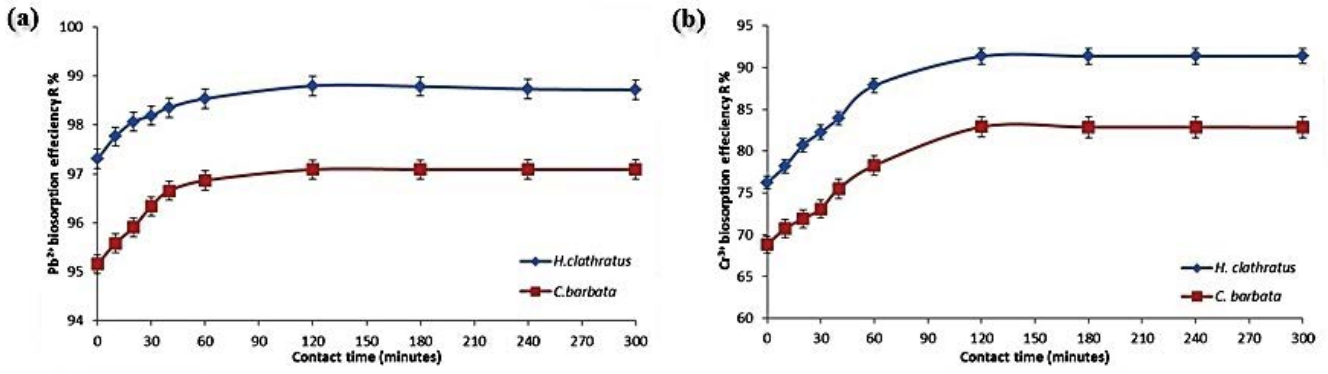

Fig. 6. Influence of reaction time on (a) Pb^{2+} and (b) Cr^{3+} biosorption efficiency R (%) of *Hydroclathrus clathratus* and *Cystoseira barbata* (T: 25°C; m: 1 g; pH: 5; and V: 100 mL). The data are the mean of three replicate readings ± SD.

The initial metal concentration produced a dynamic strength to overcome the resistance of mass transmission between the solid material and aqueous medium [9,25].

3.4. Kinetic studies of Pb^{2+} and Cr^{3+} biosorption

The kinetic analysis supply information concerning the sorption mechanism that improves the adsorption process efficiency [32]. The two rate equations of "pseudo-first-order" (Fig. 8) and the "pseudo-second-order" (Fig. 9) have been used to analyze Pb^{2+} and Cr^{3+} ions kinetic data of the biosorption process by *H. clathratus* and *C. barbata*. The mathematical equation of the pseudo-first-order model of our kinetic studies is displayed as [42]:

$$\ln\left(q_e - q_t\right) = \ln q_e - k_1 t \tag{4}$$

The representative linear relationship of $\ln(q_e - q_t)$ vs. t was figured to estimate the Lagergren pseudo-first-order

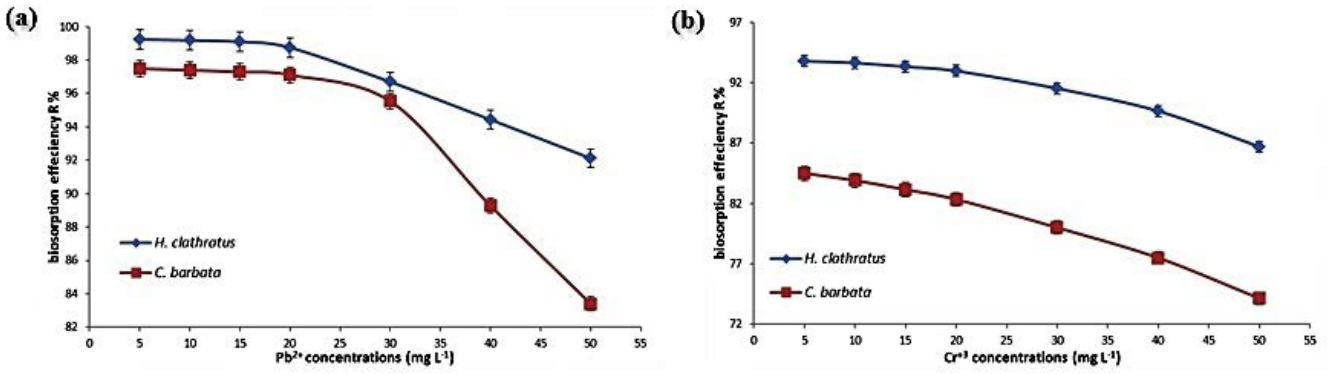

Fig. 7. Initial (a) Pb^{2+} and (b) Cr^{3+} concentrations effect on removal efficiency R (%) by *Hydroclathrus clathratus* and *Cystoseira barbata* (T: 25°C; V: 100 mL; pH: 5; and m: 1 g). The data are the mean of three replicate readings ± SD.

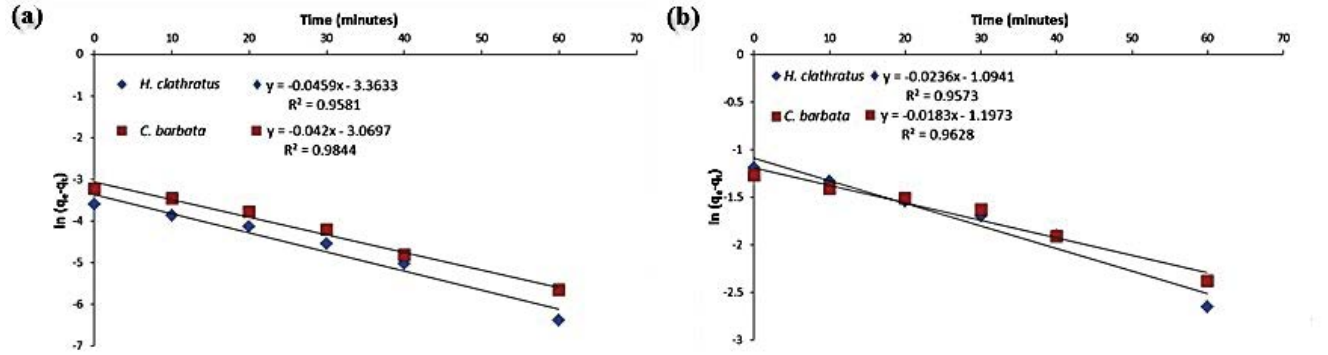

Fig. 8. Pseudo-first-order kinetic analysis for the biosorption of (a) Pb^{2+} and (b) Cr^{3+} ions onto *H. clathratus* and *C. barbata* biomass (T: 25°C; pH: 5; V: 100 mL; and m: 1 g).

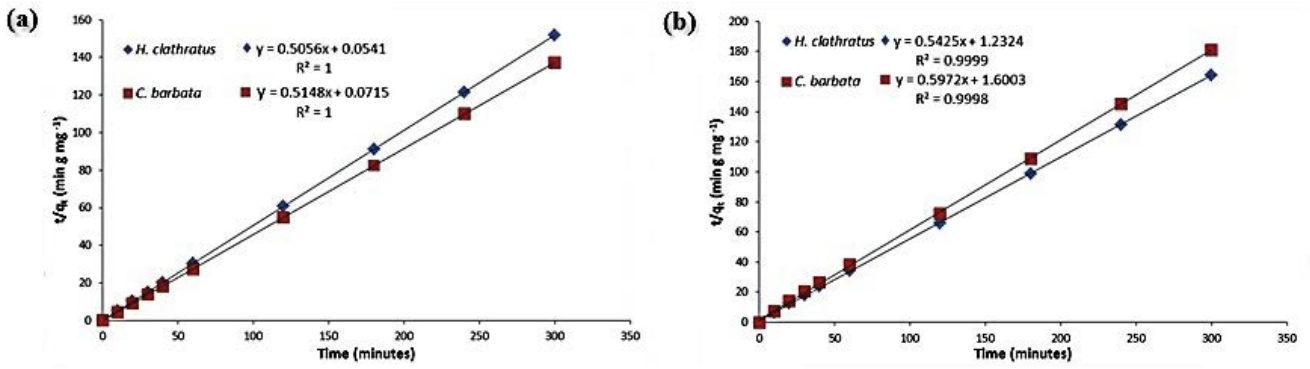

Fig. 9. Pseudo-second-order kinetic analysis for the biosorption of (a) Pb^{2+} and (b) Cr^{3+} ions onto *H. clathratus* and *C. barbata* biomass (*T*: 25°C; pH: 5; *V*: 100 mL; and *m*: 1 g).

Table 2
Pb^{2+} and Cr^{3+} biosorption parameters of pseudo-first-order and pseudo-second-order kinetic models

Kinetics parameter	Pb^{2+}		Cr^{3+}	
	H. clathratus	*C. barbata*	*H. clathratus*	*C. barbata*
$q_{e,exp}$ (mg g^{-1})	1.977	1.942	1.827	1.658
Pseudo-first-order				
R^2	0.958	0.984	0.957	0.963
$q_{e,calc}$ (mg g^{-1})	0.035	0.046	0.335	0.302
k_1 (min^{-1})	0.046	0.042	0.024	0.018
Pseudo-second-order				
R^2	1	1	0.999	0.999
$q_{e,calc}$ (mg g^{-1})	1.978	1.943	1.843	1.674
k_2 (g mg^{-1} min^{-1})	4.725	3.707	0.239	0.223
h (mg g min^{-1})	18.48	13.99	0.811	0.625

rate constant value (k_1, min^{-1}). We estimated the rate of equilibrium biosorption capacity (q_e, mg g^{-1}) after calculating the plot intercepts and slopes, given that the quantity of metal uptake on the mass unit of sorbent at time t is (q_t, mg g^{-1}).

We also analyze kinetic data of the biosorption process with linear form of pseudo-second-order mathematical equation [43] which can be written as follows:

$$\frac{t}{q_t} = \frac{1}{k_2 q_e^2} + \frac{1}{q_e} t \tag{5}$$

The mathematical equation of the initial biosorption rate can be displayed as:

$$h = k_2 q_e^2 \tag{6}$$

where k_2 is the rate constant of the pseudo-second-order at the equilibrium (g mg^{-1} min^{-1}). The linear form of t/q_t vs. t was figured and the values of k_2 and q_e were estimated.

Table 2 summarizes the parameters of biosorption kinetics together with correlation coefficient values (R^2). It is clear that the "pseudo-first-order kinetic model" presents the worst performance on describing the biosorption of Pb^{2+} and Cr^{3+}, over the entire period it was studied. The pseudo-second-order kinetic model described the experimental data very well with high correlation coefficient values ($R^2 > 0.999$).

In the "pseudo-second-order model," the estimated equilibrium capacity values ($q_{e,calc}$) are close to the experimentally determined values ($q_{e,exp}$), for investigated Pb^{2+} and Cr^{3+} metals. This indicates that the kinetic model of the pseudo-second-order was very good in characterizing the biosorption kinetics of the investigated Pb^{2+} and Cr^{3+} metals on the algal biomass. The second-order kinetic study suggests that the biosorption process occurred according to the chemical interactions between the metal ions and binding sites of the biomass surface [44].

3.5. Equilibrium biosorption isotherm studies

The isotherm studies of the biosorption process are described by specific constant values, which describe the superficial properties and the possible interactive trends between biosorbent and various metals [45]. This research employed the two most frequently applied isotherm models

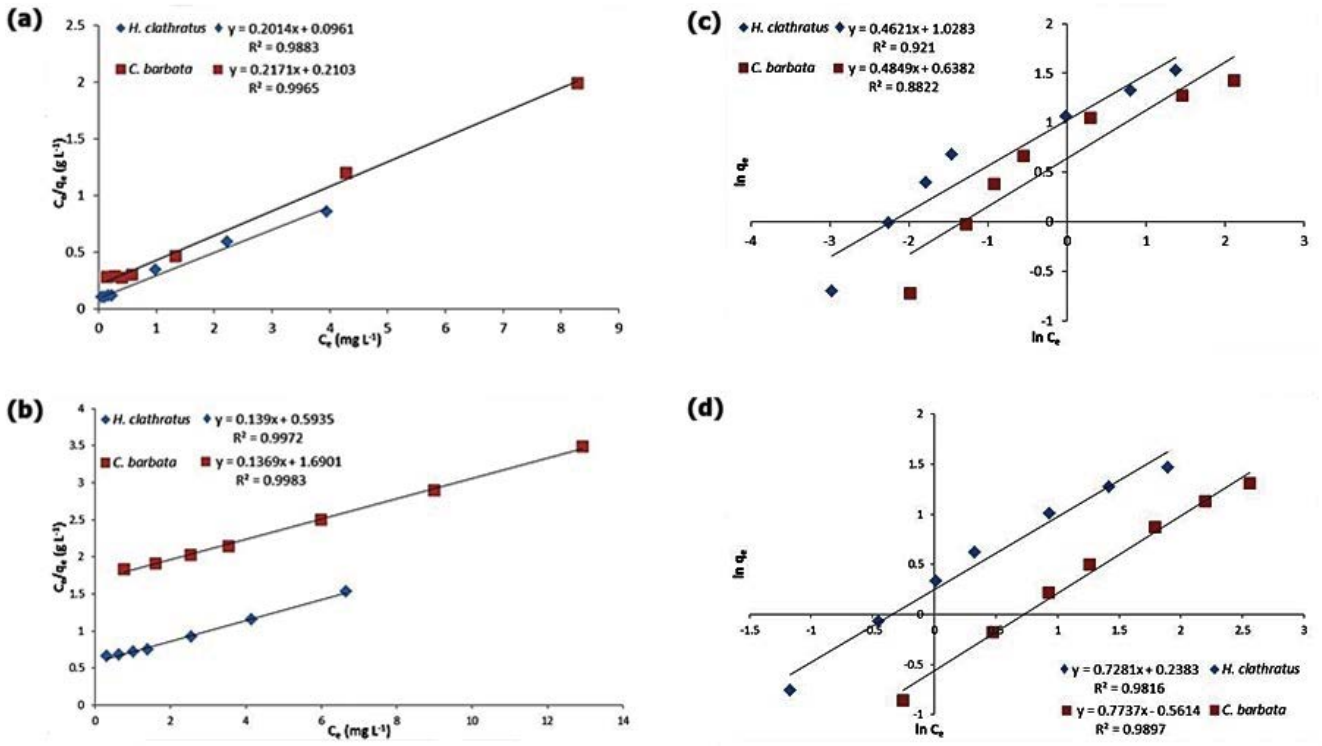

Fig. 10. Langmuir isotherm plots for the biosorption of (a) Pb^{2+} and (b) Cr^{3+} ions and Freundlich plots for the biosorption of (c) Pb^{2+} and (d) Cr^{3+} ions onto *H. clathratus* and *C. barbata* biomass (*T*: 25°C; pH: 5; *V*: 100 mL; and *m*: 1 g).

for the aqueous phase biosorption; specifically the Langmuir and Freundlich isotherm models to fit the experimental information for Pb^{2+} and Cr^{3+} ions biosorption (Fig. 10).

The Langmuir model is related to monolayer biosorption over a homogeneous surface containing a restricted number of binding sites [46]. The mathematical equation for the Langmuir model can be displayed as:

$$\frac{C_e}{q_e} = \frac{1}{q_{\max}} C_e + \frac{1}{q_{\max} K_L} \tag{7}$$

where q_e (mg g^{-1}) is the amount value of the biosorbed heavy metal per unit mass of the biosorbent at the equilibrium, C_e (mg L^{-1}) is the metal concentration at the equilibrium, $q_{\max}$ (mg g^{-1}) is the maximum possible value of biosorbed heavy metal per unit weight of the biosorbent mass and K_L is the Langmuir isotherm constant value which closely describes the affinity of the binding functional sites for heavy metals and is associated with the biosorption free energy. Langmuir parameters give useful data concerning the sorption process in terms of maximum sorption capacity ($q_{\max}$) and affinity (b) [47]. We estimated the parameters value ($q_{\max}$ and K_L) of the Langmuir model from the plot intercepts and slopes of linear plots for C_e/q_e against C_e and summarized them in Table 3.

Table 3
Constant values for the biosorption isotherms of Pb^{2+} and Cr^{3+} ions onto *H. clathratus* and *C. barbata* biomass

Isotherm parameters	Pb^{2+}		Cr^{3+}	
	H. clathratus	*C. barbata*	*H. clathratus*	*C. barbata*
Langmuir model				
R^2	0.988	0.996	0.997	0.998
$q_{\max}$ (mg g^{-1})	4.965	4.606	7.194	7.304
K_L (L mg^{-1})	2.096	1.032	0.234	0.081
Freundlich model				
R^2	0.921	0.882	0.982	0.989
N	2.164	2.062	1.373	1.292
K_F (L g^{-1})	2.796	1.893	1.269	0.570

The Freundlich isotherm is an empirical nature model which determines heterogeneous surface biosorption and is not restricted to monolayer formation. It is believed that increasing the site occupation amount will decrease the binding strength, as the first occupation occurs to the stronger binding sites [48,49]. The mathematical equation of this model can be displayed as:

$$q_e = K_F C_e^{1/n} \tag{8}$$

Rearranging Eq. (8) gives:

$$\ln q_e = \ln K_F + \frac{1}{n}\ln C_e \tag{9}$$

where K_F (L g^{-1}) is the Freundlich constant and is an indicator of the adsorption capacity and $1/n$ (dimensionless) is the parameter related to adsorption intensity. Moreover, $1/n$ value ranging between 0 and 1 and describes the surface heterogeneity. If its value gets nearer to zero, the biosorbent surface describing as more heterogeneous. The values of $1/n$ are less than one at studied metals indicating the degree of non-linearity. The values of the (R^2) show that the experimental biosorption isotherm data of considered Pb^{2+} and Cr^{3+} ions are very well described by the Langmuir isotherm model which showed that the biosorption is homogeneous due to the homogeneity of the biomass surface. The Freundlich correlation coefficient values (R^2) are lower than the Langmuir correlation coefficient values obtained. The R^2 values calculated in this study indicate that the Freundlich isotherm is insufficient to describe the Pb^{2+} and Cr^{3+} biosorption onto algal biomass.

As illustrated in Table 3, the maximum biosorption capacities (q_m) of Pb^{2+} and Cr^{3+} biosorption are 4.97, 7.19 mg g^{-1} on *H. clathratus* and 4.61, 7.30 mg g^{-1} on *C. barbata*, respectively. It is essential to analyze the equilibrium data to develop an equation that can be applied to design and optimize an operating procedure and to compare different sorbents under different operating conditions [50]. To compare q_m values with other biosorbents, Kumar et al. [51], ascertained that the Pb^{2+} uptake values for *Cladophora fasicularis* ranged from 5.68 to 33.53 mg g^{-1} and from 6.19 to 25.07 mg g^{-1} by means of green biomass *Ulva lactuca*. Additionally, the maximum biosorption capacity of Pb^{2+} by *Chaetomorpha* sp., was between 7.52 and 35.08 mg g^{-1} whilst the Pb^{2+} biosorption capacity values were in the range of 6.03 to 21.58 and 6.42 to 37.71 mg g^{-1} by *Caulerpa sertularioides* and *Valoniopsis pachynema*, respectively. Murphy et al. [47], concluded that the q_{max} values calculated for Cr^{3+} binding decreased in the order: brown (*Fucus vesiculosus*) > green > red (*Palmaria palmate*) and q_{max} value for *Ulva* spp. was 1.02 mmol g^{-1}. Tamilselvan et al. [52], reported that the q_{max} value of Cr^{3+} by *Caulerpa racemosa* was 1.13 mmol g^{-1} and that the *Sargassum wightii* (brown biomass) exhibited 78% biosorption for Pb^{2+} and Cr^{3+} ions.

4. Conclusion

The present study reveals that the parameters effects on Pb^{2+} and Cr^{3+} ions biosorption from contaminated solution utilizing the algal biomass were examined. The biosorption process is not only based on the chemical composition of biosorbent material and nature of solutes, but also strongly influenced by different factors such as reaction time, pH, biosorbent dose, and the initial concentrations of metal ions. The brown algal biomass demonstrated increased capacity for metal biosorption and that it can be used for treating certain effluents. A suitable pH value for Pb^{2+} and Cr^{3+} biosorption onto *H. clathratus* and *C. barbata* biosorbent was 5. Ten grams per liter of the biomass and was sufficient for the maximum Pb^{2+} and Cr^{3+} biosorption. The studied equilibrium isotherms for Pb^{2+} and Cr^{3+} biosorption fitted best to the Langmuir model and the pseudo-second-order kinetic equations described the Pb^{2+} and Cr^{3+} biosorption kinetics extremely well. The final contribution of our results suggests that *H. clathratus* and *C. barbata* are promising biosorbent material for Pb^{2+} and Cr^{3+} bioremoval and wastewater treatment due to its high biosorption efficiency.

Acknowledgments

The authors are extremely grateful to the Department of Ecology, Soils, Water, and Environment Research Institute (SWERI), Agriculture Research Centre (ARC), and the University of Beni-Suef for providing support to conduct this research.

Symbols

C_0	—	Initial concentration of metal ions in aqueous solution, mg L^{-1}
C_t	—	Concentration of metal ions at any time t, mg L^{-1}
C_e	—	Concentration of metal ions at equilibrium state, mg L^{-1}
K_L	—	Constant of Langmuir, L mg^{-1}
k_2	—	Constant of second-order model, g mg^{-1} min^{-1}
M	—	Mass of the adsorbent, g
$1/n$	—	Freundlich parameter
q_e	—	Equilibrium concentration in solid phase, mg g^{-1}
q_{max}	—	Maximum adsorbed amount per unit mass of adsorbent, mg g^{-1}
q_t	—	Adsorbed amount at time t, mg g^{-1}
t	—	Time, min

References

[1] S. Rangabhashiyam, P. Balasubramanian, Biosorption of hexavalent chromium and malachite green from aqueous effluents, using *Cladophora* sp., J. Chem. Ecol., 34 (2018) 371–390.
[2] M.K. Uddin, A review on the adsorption of heavy metals by clay minerals, with special focus on the past decade, J. Chem. Eng., 308 (2017) 438–462.
[3] R. Jalali, H. Ghafourian, Y. Asef, S.J. Davarpanah, S. Sepehr, Removal and recovery of lead using nonliving biomass of marine algae, J. Hazard. Mater., 92 (2002) 253–262.
[4] R. Dabbagh, M. Ebrahimi, F. Aflaki, H. Ghafourian, M.H. Sahafipour, Biosorption of stable cesium by chemically modified biomass of *Sargassum glaucescens* and *Cystoseira indica* in a continuous flow system, J. Hazard. Mater., 159 (2008) 354–357.
[5] P. Arivalagan, D. Singaraj, V. Haridass, T. Kaliannan, Removal of cadmium from aqueous solution by batch studies using *Bacillus cereus*, J. Ecol. Eng., 71 (2014) 728–735.
[6] A.M. Taiwo, A.M. Gbadebo, J.A. Oyedepo, Z.O. Ojekunle, O.M. Alo, A.A. Oyeniran, O.J. Onalaja, D. Ogunjimi, O.T. Taiwo,

Bioremediation of industrially contaminated soil using compost and plant technology, J. Hazard. Mater., 304 (2016) 166–172.
[7] A.M. Abdel-Satar, M.H. Ali, M.E. Goher, Indices of water quality and metal pollution of Nile River, Egypt, Egypt. J. Aquat. Res., 43 (2017) 21–29.
[8] Y. Al Naggar, M.S. Khalil, M.A. Ghorab, Environmental pollution by heavy metals in the aquatic ecosystems of Egypt, J. Toxicol., 3 (2018), doi: 10.19080/OAJT.2018.03.555603.
[9] H. Pahlavanzadeh, A.R. Keshtkarb, J. Safdarib, Z. Abadia, Biosorption of nickel(II) from aqueous solution by brown algae: equilibrium, dynamic and thermodynamic studies, J. Hazard. Mater., 175 (2010) 304–310.
[10] P. Kumar, K.H. Kim, V. Bansal, T. Lazarides, N. Kumar, Progress in the sensing techniques for heavy metal ions using nanomaterials, J. Ind. Eng. Chem., 54 (2017) 30–43.
[11] J.M. Jacob, C. Karthik, R.G. Saratale, S.S. Kumar, D. Prabakar, K. Kadirvelu, A. Pugazhendhi, Biological approaches to tackle heavy metal pollution: a survey of literature, J. Environ. Manage., 217 (2018) 56–70.
[12] D. Park, Y.-S. Yun, D.S. Lee, J.M. Park, Optimum condition for the removal of Cr(VI) or total Cr using dried leaves of *Pinus densiflora*, Desalination, 271 (2011) 309–314.
[13] J. Kyzioł-Komosinska, J. Augustynowicz, W. Lasek, J. Czupioł, D. Ocinski, *Callitriche cophocarpa* biomass as a potential low-cost biosorbent for trivalent chromium, J. Environ. Manage., 214 (2018) 295–304.
[14] R. Mohamed, H.H. El-Maghrabi, M. Riad, S. Mikhail, Environmental friendly FeOOH adsorbent materials preparation, characterization and mathematical kinetics adsorption data, J. Water Process Eng., 16 (2017) 212–222.
[15] L.C. Oliveira, W.G. Botero, T.S. Farias, J.C.C. Santos, G.V.M. Gabriel, D. Goveia, T.A. Cacuro, W.R. Waldman, Application of natural organic residues as adsorbents to remove lead from waters, J. Water Air Soil Pollut., 230 (2019) 191, doi: 10.1007/s11270–019–4240–8.
[16] Y. Hannachi, A. Rezgui, A.B. Dekhil, T. Boubaker, Removal of cadmium(II) from aqueous solutions by biosorption onto the brown macroalga (*Dictyota dichotoma*), Desal. Water Treat., 54 (2015) 1663–1673.
[17] A.K. Zeraatkar, H. Ahmadzadeh, A.F. Talebi, N.R. Moheimani, M.P. McHenry, Potential use of algae for heavy metal bioremediation, a critical review, J. Environ. Manage., 181 (2016) 817–831.
[18] F. Deniz, A. Karabulut, Biosorption of heavy metal ions by chemically modified biomass of coastal seaweed community: studies on phycoremediation system modeling and design, J. Ecol. Eng., 106 (2017) 101–108.
[19] B. Henriques, L.S. Rocha, C.B. Lopes, P. Figueira, A.C. Duarte, C. Vale, M.A. Pardal, E. Pereira, A macroalgae-based biotechnology for water remediation: simultaneous removal of Cd, Pb and Hg by living *Ulva lactuca*, J. Environ. Manage., 191 (2017) 275–289.
[20] K.K.A. Sanjeewa, E.-A. Kim, K.-T. Son, Y.-J. Jeon, Bioactive properties and potentials cosmeceutical applications of phlorotannins isolated from brown seaweeds: a review, J. Photochem. Photobiol., B, 162 (2016) 100–105.
[21] K. Vijayaraghavan, S. Rangabhashiyam, T. Ashokkumar, J. Arockiaraj, Assessment of samarium biosorption from aqueous solution by brown macroalga *Turbinaria conoides*, J. Taiwan Inst. Chem. Eng., 74 (2017) 113–120.
[22] L.P. Mazur, M.A.P. Cechinel, S.M.A. Souza, R.A.R. Boaventura, V.J.P. Vilar, Brown marine macroalgae as natural cation exchangers for toxic metal removal from industrial wastewaters: a review, J. Environ. Manage., 223 (2018) 215–253.
[23] T.A. Davis, B. Volesky, A. Mucci, A review of the biochemistry of heavy metal biosorption by brown algae, J. Water Res., 37 (2003) 4311–4330.
[24] A. Sari, O.D. Uluozlü, M. Tuzen, Equilibrium, thermodynamic and kinetic investigations on biosorption of arsenic from aqueous solution by algae (*Maugeotia genuflexa*) biomass, J. Chem. Eng., 167 (2011) 155–161.
[25] L. Vafajoo, R. Cheraghi, R. Dabbagh, G. McKay, Removal of cobalt(II) ions from aqueous solutions utilizing the pre-treated 2-Hypnea Valentiae algae: equilibrium, thermodynamic, and dynamic studies, J. Chem. Eng., 331 (2018) 39–47.
[26] M. El-Sheekh, S. El Sabagh, G. Abou El-Souod, A. Elbeltagy, Biosorption of cadmium from aqueous solution by free and immobilised dry biomass of *Chlorella vulgaris*, Int. J. Environ. Res., 13 (2019) 511–521.
[27] Z. Lou, J. Wang, X. Jin, L. Wan, Y. Wang, H. Chen, W. Shan, Y. Xiong, Brown algae based new sorption material for fractional recovery of molybdenum and rhenium from wastewater, J. Chem. Eng., 273 (2015) 231–239.
[28] L.M.T. Rosa, W.G. Botero, J.C.C. Santos, T.A. Cacuro, W.R. Waldman, J.B. Carmo, L.C. Oliveira, Natural organic matter residue as a low cost adsorbent for aluminium, J. Environ. Manage., 215 (2018) 91–99.
[29] R.B. Nessim, A.R. Bassiouny, H.R. Zaki, M.N. Moawad, K.M. Kandeel, Biosorption of lead and cadmium using marine algae, J. Chem. Ecol., 27 (2011) 579–594.
[30] T.A. Pozdniakova, L.P. Mazur, R.A.R. Boaventura, V.J.P. Vilar, Brown macro-algae as natural cation exchangers for the treatment of zinc containing wastewaters generated in the galvanizing process, J. Cleaner Prod., 119 (2016) 38–49.
[31] B. Sarada, M.K. Prasad, K.K. Kumar, C.V.R. Murthy, Potential use of *Caulerpa fastigiata* biomass for removal of lead: kinetics, isotherms, thermodynamic and characterization studies, Environ. Sci. Pollut. Res. Int., 21 (2014) 1314–1325, doi: 10.1007/s11356-013-2008-z.
[32] S.T. Akar, S. Arslan, T. Alp, D. Arslan, T. Akar, Biosorption potential of the waste biomaterial obtained from *Cucumis melo* for the removal of Pb^{2+} ions from aqueous media: equilibrium, kinetic, thermodynamic and mechanism analysis, J. Chem. Eng., 185–186 (2012) 82–90.
[33] K.S. Tong, M.G. Kassim, A. Azra, Adsorption of copper ion from its aqueous solution by a novel biosorbent *Uncaria gambir*: equilibrium, kinetics, and thermodynamic studies, J. Chem. Eng., 170 (2011) 145–153.
[34] A. Verma, S. Kumar, S. Kumar, Biosorption of lead ions from the aqueous solution by *Sargassum filipendula*: equilibrium and kinetic studies, J. Environ. Chem. Eng., 4 (2016) 4587–4599.
[35] F.V. Hackbarth, F. Girardi, S.M.A.G.U. de Souza, A.A.U. de Souza, R.A.R. Boaventura, V.J.P. Vilar, Marine macroalgae *Pelvetia canaliculata* (Phaeophyceae) as a natural cation exchanger for cadmium and lead ions separation in aqueous solutions, J. Chem. Eng., 242 (2014) 294–305.
[36] N.A. Negm, M.G. Abd El Wahed, A.R.A. Hassan, M.T.H. Abou Kana, Feasibility of metal adsorption using brown algae and fungi: effect of biosorbents structure on adsorption isotherm and kinetics, J. Mol. Liq., 264 (2018) 292–305.
[37] M.A. Badawi, N.A. Negm, M.T.H. Abou Kana, H.H. Hefni, M.M. Abdel Moneem, Adsorption of aluminium and lead from wastewater by chitosan-tannic acid modified biopolymers: isotherms, kinetics, thermodynamics and process mechanism, Int. J. Biol. Macromol., 99 (2017) 465–476.
[38] W.M. Ibrahim, Biosorption of heavy metal ions from aqueous solution by red macroalgae, J. Hazard. Mater., 192 (2011) 1827–1835.
[39] S.C.R. Santos, G. Ungureanu, I. Volf, R.A.R. Boaventura, C.M.S. Botelho, Macroalgae Biomass As Sorbent For Metal Ions, V. Popa, I. Volf, Eds., Biomass as Renewable Raw Material to Obtain Bioproducts of High-Tech Value, Woodhead Publishing, Cambridge, UK, 2018, pp. 69–112.
[40] X. Han, Y.S. Wong, N.F. Tam, Surface complexation mechanism and modeling in Cr(III) biosorption by a microalgal isolate, *Chlorella miniata*, J. Colloid Interface Sci., 303 (2006) 365–371.
[41] T. Akar, Z. Kaynak, S. Ulusoy, D. Yuvaci, G. Ozsari, G.S.T. Akar, Enhanced biosorption of nickel(II) ions by silica-gel-immobilized waste biomass: biosorption characteristics in batch and dynamic flow mode, J. Hazard. Mater., 163 (2009) 1134–1141.
[42] S. Lagergren, Zur theorie der sogenannten adsorption geloster stoffe, Kungl. Sven. Vetenskapsakad. Handl., 24 (1898) 1–39.
[43] Y.S. Ho, G. McKay, Kinetic models for the sorption of dye from aqueous solution by wood, J. Process Saf. Environ., 76 (1998) 183–191.

[44] D. Bulgariu, L. Bulgariu, Equilibrium and kinetics studies of heavy metal ions biosorption on green algae waste biomass, J. Bioresour. Technol., 103 (2012) 489–493.
[45] A.M. Motawie, K.F. Mahmoud, A.A. El-Sawy, H.M. Kamal, H.H. Hefni, H.A. Ibrahiem, Preparation of chitosan from the shrimp shells and its application for pre-concentration of uranium after cross-linking with epichlorohydrin, Egypt. J. Pet., 23 (2014) 221–228.
[46] I. Langmuir, The adsorption of gases on plane surfaces of glass, mica and platinum, J. Am. Chem. Soc., 40 (1918) 1361–1403.
[47] V. Murphy, H. Hughes, P. McLoughlin, Comparative study of chromium biosorption by red, green and brown seaweed biomass, Chemosphere, 70 (2008) 1128–1134.
[48] H.M.F. Freundlich, Over the adsorption in solution, J. Phys. Chem., 57 (1906) 385–470.
[49] B. Akduman, M. Uygun, D.A. Uygun, S. Akgöl, A. Denizli, Purification of yeast alcohol dehydrogenase by using immobilized metal affinity cryogels, J. Mater. Sci. Eng., 33 (2013) 4842–4848.
[50] Y. Khambhaty, K. Mody, S. Basha, B. Jha, Kinetics, equilibrium and thermodynamic studies on biosorption of hexavalent chromium by dead fungal biomass of marine *Aspergillus niger*, J. Chem. Eng., 145 (2009) 489–495.
[51] J.I.N. Kumar, C. Oommen, R.N. Kumar, Biosorption of heavy metals from aqueous solution by green marine macroalgae from Okha Port, Gulf of Kutch, India Am.-Eurasian J. Agric. Environ. Sci., 6 (2009) 317–323.
[52] N. Tamilselvan, K. Saurav, K. Kannabiran, Biosorption of Cr(VI), Cr(III), Pb(II) and Cd(II) from aqueous solutions by *Sargassum wightii* and *Caulerpa racemosa* algal biomass, J. Ocean Univ. China, 11 (2012) 52–58.
[53] S. Yalçın, S. Sezer, R. Apak, Characterization and lead(II), cadmium(II), nickel(II) biosorption of dried marine brown macro algae *Cystoseira barbata*, Environ. Sci. Pollut. Res., 19 (2012) 3118–3125.
[54] V. Murphy, H. Hughes, P. McLoughlin, Copper binding by dried biomass of red, green and brown macroalgae, J. Water Res., 41 (2007) 731–740.